

# Atypical Wavelet Descriptor of Curves Using Principal Components

Vignesh D <sup>a</sup>, Palanisamy T <sup>b</sup>

<sup>a,b</sup> *Department of Mathematics, Amrita School of Physical Sciences Coimbatore,  
Amrita Vishwa Vidyapeetham, Tamil Nadu 641112, India*

**Abstract:** The relationship between the sample points of a space curve and scaled, rotated and translated sample points are often not evident either geometrically or analytically. However the research fraternity working on linkage mechanism found this relationship useful for their study which they captured through Fourier and wavelet transforms. It is significant to observe that most of the research works carried out is pertaining to planar curves. Further the strategy adapted for the planar curve is not suitable for the curves in space. This challenge of extracting relationship between both the sets of sample points of the space curve motivates the authors to suitably reduce the dimension and proceed. In our proposed work the Principal Component Analysis (PCA) is used to reduce the dimension of the sample points of the space curve to the points on a plane. It is interesting to note that the desired relationship is found to be present in a specific ratio of atypical wavelet detailed coefficients of the points obtained by dimensional reduction. The results are also supported by illustrating examples of continuous curves.

**Keywords:** Space curves, Sample points, PCA, Atypical wavelet transform, Invariant feature vector.

## 1. Introduction

The four bar linking system is the subject of numerous investigations. Cartesian coordinates are employed in the case of planar four bar linkages in studies of this issue, but spherical coordinates were used in the case of a four bar linkage mechanism involving a space curve. All of these studies make an effort to unearth the hidden connections between members of the same family of curves that exhibit comparable geometric properties. After expressing the planar curve by its Fourier coefficients, different attempts have been made to create the feature vector that is invariant under scaling, translation, and rotation.

For the convenience of readers, a few of these studies on the Fourier based four bar connection mechanism are described here. Freudenstien, McGarva [4, 10, 11] have represented the coupler curve in Four bar mechanism using Fourier coefficients with the discussion of the geometric significance of harmonic terms. On the basis of normalised Fourier coefficients, McGava [12] and Mullineux [13] obtained catalogues. Sun [17] suggested a three-dimensional Fourier series for the analysis of coupler curves. Wu uses the Fourier series to efficiently depict the coupler curve [22, 23]. The Fourier coefficients are appropriate for periodic curves, however it is unavoidable to analyse open curves in numerous problems. This

prompts Uesaka to propose the new Fourier description for open curves [20]. Despite this effort Liu et al. [8] proved there are certain limitations [1] to use Fourier series on the open curves and hence wavelet coefficient descriptors of open non-periodic curves were obtained by them. There is also a study using wavelet coefficient descriptors for the space curves based on spherical coordinate system [18].

It is significant to state that there are studies exclusively on the plane and space curves independent of curves associated to linkage mechanism using wavelet descriptors. In order to describe a plane closed curve that is invariant during scaling, translation, and rotation, Hung et al. proposed the wavelet descriptor [6]. They also illustrated that the proposed descriptor can be used as a feature for pattern recognition. Teing et al. developed an algorithm [19] for representing the space curves that are invariant under scaling, translation and rotation.

The proposed work attempts to study invariance properties of curves in space represented in Cartesian system. Liu et al. [8] and in their attempt found the invariance property of the planar curves using the wavelet detailed coefficients. In fact, the ratios of the pair of wavelet detailed coefficients are found to be invariant. But it is to be noted that the

computation of the ratio became possible by considering them as complex numbers [21]. Thus the computation of the ratio used by Liu et al. [8] can never be accomplished for space curves. Therefore in the proposed article we extract the invariance property of the space curves using PCA. Thus, in this article we propose a transformation invariant feature vector (TIFV) based on the wavelet coefficients of the sample points of the space curve. The organisation of the rest of this paper is as follows: Section 2. briefly gives some background on wavelets and principal component analysis. The proposed work is discussed in Section 3. The illustrated examples are presented in Section 4. The paper concludes with Section 5.

## 2. Review

### 2.1 Waveletes

In this section, we give a brief exposition of the wavelet theory which is desirable in various engineering problems [5] including curve description. The wavelet transform of a function  $f(x)$  in  $L^2(\mathbb{R})$  is the representation of it using a family of orthonormal bases of the form  $\psi_{j,k}(x) = 2^{j/2}\psi(2^jx - k)$  obtained through translation and dilation of some  $\psi(x)$  belongs to  $L^2(\mathbb{R})$ , known as the mother wavelet [3, 16].

For this purpose, Mallat determined a set of properties that a sequence of embedded vector spaces  $\{V_j\}_{j \in \mathbb{Z}}$  should have. With these properties the sequence becomes the Multiresolution Analysis (MRA) which in turn will yield a compactly supported wavelet system and the definition of MRA is as follows [3].

**Definition 1.** A MRA with scaling function  $\varphi$  is a sequence  $\{V_j\}_{j \in \mathbb{Z}}$  of subspaces of  $L^2(\mathbb{R})$  having the following properties:

- (i) The sequence is increasing, that is,  $V_j \subseteq V_{j+1}$  for all  $j \in \mathbb{Z}$ .
- (ii) There exists a function  $\varphi \in V_0$  such that the set  $\{\varphi_{0,k}\}_{k \in \mathbb{Z}}$  is orthonormal and  $V_0 = \{\sum_{k \in \mathbb{Z}} z(k)\varphi_{0,k} : z = (z(k))_{k \in \mathbb{Z}}\}$
- (iii) For each  $j$ ,  $f(x) \in V_0$  iff  $f(2^jx) \in V_j$ .
- (iv)  $\bigcap_{j \in \mathbb{Z}} V_j = \{0\}$  and
- (v)  $\bigcup_{j \in \mathbb{Z}} V_j$  is dense in  $L^2(\mathbb{R})$ .

We describe here the interesting development of the discovery of compactly supported orthonormal bases of wavelets by Daubechies [4]. The function  $\varphi \in L^2(\mathbb{R})$  given in Definition 2.1 is considered for

the discussion and we use  $\varphi_{j,k}(x)$  to denote  $2^{j/2}\varphi(2^jx - k)$  for some  $j, k \in \mathbb{Z}$ .

If  $\{\varphi_{1,k} = \sqrt{2}\varphi(2x - k) : k \in \mathbb{Z}\}$  is a complete orthonormal set in  $V_1$  for some  $\varphi \in V_0$ , by the property (i) of Definition 2.1 we can express  $\varphi = \sum_{k \in \mathbb{Z}} u(k)\varphi_{1,k}$  [7]. This is known as scaling equation or refinement relationship of  $\varphi$ . Further, if we are able to find the solution  $\mathbf{u} = (u(k))_{k \in \mathbb{Z}}$  and  $\varphi$  of the scaling equation such that  $\int_{\mathbb{R}} \varphi(t)dt = 1$ , then the properties of MRA will be satisfied by the embedded vector spaces  $\{V_j\}_{j \in \mathbb{Z}}$  generated by  $\{\varphi_{j,k}\}_{j,k \in \mathbb{Z}}$ . Based on the relationship of the nested subspaces of MRA, it is natural to ask what are the elements in  $V_1$  that are not in  $V_0$ ? This is the vital question which gives birth to the basis functions of  $L^2(\mathbb{R})$ . If  $\mathbf{u} \in l^2(\mathbb{Z})$ , the space of all square summable sequences, and  $R_{2k}(u) = (u(n - 2k))_{n \in \mathbb{Z}}$  for some integer  $k$  such that  $\{R_{2k}(u)\}_{k \in \mathbb{Z}}$  is orthonormal in  $l^2(\mathbb{Z})$  then  $\{R_{2k}(u) \cup R_{2k}(v)\}_{k \in \mathbb{Z}}$  is an orthonormal basis for  $l^2(\mathbb{Z})$  where  $\mathbf{v} = \{v(k) : v(k) = (-1)^k u(1 - k)\}$ .

Letting

$$\psi(x) = \sum_{k \in \mathbb{Z}} v(k)\varphi_{1,k}$$

and

$$W_0 = \left\{ \sum_{k \in \mathbb{Z}} z(k)\psi_{0,k} : z \in l^2(\mathbb{Z}) \right\}$$

we can easily see that  $\{\psi(x - k) : k \in \mathbb{Z}\}$  is orthonormal to  $\{\varphi(x - k) : k \in \mathbb{Z}\}$ . This  $W_0$  is the searched complement of  $V_0$  in  $V_1$  and is obviously orthonormal to  $V_0$  and hence  $V_1 = V_0 \oplus W_0$ . If  $W_j$  is the subspace spanned by  $\{2^{j/2}\psi(2^jx - k) : k \in \mathbb{Z}\}$  then it can be shown that  $W_j$  is orthogonal complement of  $V_j$  in  $V_{j+1}$  for every  $j \in \mathbb{Z}$ . Obviously,  $W_j$ 's are not nested but  $\dots \perp W_0 \perp W_1 \perp \dots$  and as a result we have  $L^2(\mathbb{R}) = \bigoplus_{j \in \mathbb{Z}} W_j$  and

$$V_n = V_m \bigoplus_{j=m}^{\infty} W_j \quad \text{for } m < n. \quad \text{Therefore,}$$

$\{2^{j/2}\psi(2^jx - k) : j, k \in \mathbb{Z}\}$  forms an orthonormal basis for  $L^2(\mathbb{R})$ . Thus the MRA yields eventually an orthonormal basis which consists of functions known as wavelets. The projection of any function of  $L^2(\mathbb{R})$  in  $V_j$  can be thought of as the approximation of that function in the subspace  $V_j$  and the projection over  $W_j$  gives the detail to go

over to the next approximation level in  $V_{j+1}$ . This enables us to view any function of  $L^2(\mathbb{R})$  in various resolutions.

The subspaces  $V_j$ 's and  $W_j$ 's in this context are usually called as approximation and detail spaces respectively. We understand that in the discussion made above the approximation space in each level is decomposed into the next coarser level approximation space and the corresponding detail space. Further it has to be noticed that the detail space in every level is left as it is. This is the conventional wavelet decomposition and this involves a pyramid (binary tree)structured decomposition.

In the above process of constructing wavelet basis for  $L^2(\mathbb{R})$  we obtained an orthonormal set of vectors  $\{R_{2k}(u)\}_{k \in \mathbb{Z}}$  where the coordinates of  $\mathbf{u}$  are coefficients of the scaling equation. Also it is discussed about  $\{R_{2k}(v)\}_{k \in \mathbb{Z}}$  where the vector  $\mathbf{v}$  is formed by using the scaling vector  $\mathbf{u}$ . Infact, the wavelet basis for  $L^2(\mathbb{Z})$  is the orthonormal basis formed by  $\{R_{2k}(u) \cup R_{2k}(v)\}_{k \in \mathbb{Z}}$ .  $R_{2k}(u)$  and  $R_{2k}(v)$  are understood to constitute approximations and details of the given vector.

By the construction of wavelet basis it is evident that the sum of the approximation and detail at  $j^{th}$  level  $P_{-j}(\mathbf{z}) + Q_{-j}(\mathbf{z})$  will result it the approximation  $P_{-j+1}(\mathbf{z})$  at  $j + 1^{th}$  level. Inductively we can get  $\mathbf{z} = P_{-1}(\mathbf{z}) + Q_{-1}(\mathbf{z}) = P_{-2}(\mathbf{z}) + Q_{-2}(\mathbf{z}) + Q_{-1}(\mathbf{z})$  and so on until  $\mathbf{z} = P_{-j}(\mathbf{z}) + \sum_{l=1}^j Q_{-l}(\mathbf{z})$ . It is quit evident from the above discussion that the wavelet transform of any given level can be associated to a matrix [15]. We denote the matrix for  $N^{th}$  level wavelet transform by  $W_N$ . The above procedure is used in next section to obtain the wavelet transform of the collection of sample points for the given parametric curve to describe the TIFV.

### 2.2 Principal component analysis

Principal component analysis involves the selection of a new coordinate system obtained by rotating the original system. The new axes represent the directions with maximum variability and provide a simpler and more parsimonious description of the relationship between the components of the considered vectors [12]. The wavelet transform of the sample points of the space curve will not result the required TIFV as we

have done in planar curves and is found that this is due to rotation. To overcome this inability we represent the sample points of a space curve by its principal components before obtaining the wavelet transform. We discuss the proposed TIFV for the space curve in the next section.

### 3. Proposed work

We consider a parametric curve  $\mathbf{r}(t) = (x_1(t), x_2(t), x_3(t))$  in  $\mathbf{R}^3$ . Let  $\mathbf{r}(t_i) = [x_1(t_i), x_2(t_i), x_3(t_i)]^T$  for  $i = 1, 2, \dots, n$  where  $n = 2^N$  be the sample points of the curve  $\mathbf{r}(t)$  obtained by choosing values  $t_i$  of the parameter  $t$ . Let us consider  $P = [\mathbf{r}(t_1) \ : \ \mathbf{r}(t_2) \ : \ \dots \ : \ \mathbf{r}(t_n)]$  be the matrix consisting of sample points in columns.

Let the matrix  $\phi$  of size  $3 \times 2$  projects the given  $n$  observations of three dimensions into  $n$  observations on the subspace spanned by first two principal directions. Let us denote Let us denote  $P^T \phi = Q = [\mathbf{u}(t_1) \ : \ \mathbf{u}(t_2) \ : \ \dots \ : \ \mathbf{u}(t_n)]$  where  $\mathbf{u}(t_i) = [y_1(t_i), y_2(t_i)]^T$ .

We obtain the componentwise wavelet transform of the  $\{\mathbf{u}(t_i), i = 1, 2, \dots, n\}$  after which we collect the pairs of wavelet coefficients in order. For this purpose we define  $\mathbf{v}_j = (y_j(t_1), y_j(t_2), \dots, y_j(t_n))^T$  for  $j = 1, 2$ . Then the  $k^{th}$  level wavelet transform  $w_k(\mathbf{v}_j)$  of  $\mathbf{v}_j$ , for  $k = 1, 2, \dots, N$  and  $j = 1, 2$  is

$$w_k(\mathbf{v}_j) = (a_{j(k,1)}, \dots, a_{j(k, \frac{n}{2^k})}, d_{j(k,1)}, \dots, d_{j(k, \frac{n}{2^k})}, \dots, d_{j(1,1)}, \dots, d_{j(1, \frac{n}{2})})$$

In fact,  $w_k(\mathbf{v}_j) = \sum_{m=1}^{\frac{n}{2^k}} \langle \mathbf{v}_j, \phi_{-k,m} \rangle \phi_{-k,m} + \sum_{l=1}^k \sum_{m=1}^{\frac{n}{2^k}} \langle \mathbf{v}_j, \psi_{-l,m} \rangle \psi_{-l,m}$  where  $\langle \mathbf{v}_j, \phi_{-k,m} \rangle = a_{j(k,m)}$  and  $\langle \mathbf{v}_j, \psi_{-l,m} \rangle = d_{j(l,m)}$ . Here  $\phi$  and  $\psi$  will stand for the father and mother wavelet of the wavelet system we prefer for the proposed work.

We consider the following pairs of componentwise wavelet coefficients  $\mathbf{w}_{a_k,p}$  which is taken in order. It is felt essential that the readers have to cognize the significance of this representation for the purpose of our proposed work. This can otherwise be thought of as an atypical wavelet transform of the collection of principal components  $\{\mathbf{u} = \mathbf{u}(t_i), i = 1, 2, \dots, n\}$ . Thus the  $k^{th}$  level wavelet transform  $w_k(\mathbf{u})$  of the curve can be had as

$$w_k(\mathbf{u}) = (\mathbf{w}_{a_{k,1}}, \dots, \mathbf{w}_{a_{k, \frac{n}{2^k}}}, \mathbf{w}_{d_{k,1}}, \mathbf{w}_{d_{k,2}}, \dots, \mathbf{w}_{d_{k, \frac{n}{2^k}}}, \dots, \mathbf{w}_{d_{1,1}}, \mathbf{w}_{d_{1,2}}, \dots, \mathbf{w}_{d_{1, \frac{n}{2}}})$$

where  $\mathbf{w}_{a_{k,p}} = (a_{1(k,p)}, a_{2(k,p)})^T$  for  $p = 1, 2, \dots, \frac{n}{2^k}$ , and  $\mathbf{w}_{d_{q,p}} = (d_{1(q,p)}, d_{2(q,p)})^T$ , where  $q = 1, 2, \dots, N$  and  $p = 1, 2, \dots, \frac{n}{2^q}$  for every  $q$ .

Nevertheless, the fact that we use the unconventional wavelet transform for our study, it is interesting to note that it can also be represented by using the  $N$ th level wavelet transform matrix a

$$(W_N Q^T)^T = \begin{bmatrix} W_N(\mathbf{v}_1) & \vdots & W_N(\mathbf{v}_2) \\ \vdots & & \vdots \\ \mathbf{w}_{a_{N,1}} & \vdots & \mathbf{w}_{d_{N,1}} & \vdots & \dots & \vdots & \mathbf{w}_{d_{1, \frac{n}{2}}} \end{bmatrix}$$

$$= \begin{bmatrix} a_{1(N,1)} & d_{1(N,1)} & \dots & d_{1(1, \frac{n}{2})} \\ a_{2(N,1)} & d_{2(N,1)} & \dots & d_{2(1, \frac{n}{2})} \\ \vdots & \vdots & \ddots & \vdots \end{bmatrix}$$

It is understood to be essential that to explore the intrinsic relationship between the sample points of the actual curve and the transformed sample points using scaling, rotation and translation to obtain the proposed TIFV of space curve. Infact, the transformed sample points can be represented

$$\text{by } \tilde{P} = (S \circ R_\theta \circ M)P, \text{ where } S = \begin{bmatrix} s & 0 & 0 \\ 0 & s & 0 \\ 0 & 0 & s \end{bmatrix}$$

represents the scaling

$$R_\theta = R_z(\alpha)R_y(\beta)R_x(\gamma) =$$

$$\begin{bmatrix} \cos\alpha\cos\beta & \cos\alpha\sin\beta\sin\gamma - \sin\alpha\cos\gamma & \cos\alpha\sin\beta\cos\gamma + \sin\alpha\sin\gamma \\ \sin\alpha\cos\beta & \sin\alpha\sin\beta\sin\gamma + \cos\alpha\cos\gamma & \sin\alpha\sin\beta\cos\gamma - \cos\alpha\sin\gamma \\ -\sin\beta & \cos\beta\sin\gamma & \cos\beta\cos\gamma \end{bmatrix}$$

represents the rotation whose yaw, pitch and roll angles are  $\alpha, \beta, \gamma$  about axis  $z, y, x$  and  $M =$

$$\begin{bmatrix} t_x & t_x & \dots & t_x \\ t_y & t_y & \dots & t_y \\ t_z & t_z & \dots & t_z \end{bmatrix}_{3 \times n}$$

represents the translation of  $(x_i, y_i, z_i)$  to  $(x_i + t_x, y_i + t_y, z_i + t_z)$  for  $i = 1, 2, \dots, n$ .

Further we mean  $S \circ P = SP$ ,  $R_\theta \circ P = R_\theta P$  and  $M \circ P = P + M^T$ . Now we consider the wavelet transform of principal component of the transformed sample points  $W_N \tilde{Q}^T = W_N(\tilde{P}^T \tilde{\phi}) = W_N(SR_\theta P + M^T)^T \tilde{\phi} = W_N((SR_\theta P)^T \tilde{\phi} + M \tilde{\phi}) = W_N(P^T(SR_\theta)^T R_\theta \phi + M \tilde{\phi}) = W_N(P^T S^T R_\theta^T R_\theta \phi + M \tilde{\phi})$

$$= W_N P^T S \phi + W_N M \tilde{\phi}$$

Let us denote the resulting coefficients of atypical wavelet transform of the transformed sample points as  $(W_N \tilde{Q}^T)^T =$

$$\begin{bmatrix} \tilde{a}_{1(N,1)} & \tilde{d}_{1(N,1)} & \dots & \tilde{d}_{1(1, \frac{n}{2})} \\ \tilde{a}_{2(N,1)} & \tilde{d}_{2(N,1)} & \dots & \tilde{d}_{2(1, \frac{n}{2})} \\ \vdots & \vdots & \ddots & \vdots \\ \tilde{w}_{a_{N,1}} & \tilde{w}_{d_{N,1}} & \dots & \tilde{w}_{d_{1, \frac{n}{2}}} \end{bmatrix}$$

It is easy to understand that the first row of  $W_N \tilde{Q}^T$  has the influence of scaling and translation but the remaining rows have the influence of scaling only. This become possible due to rotation invariance property under principal component representation of vectors and shifting invariance property under wavelet transform. By denoting the normalized wavelet detailed vectors  $\mathbf{f} = \frac{w_{d_{q,p}}}{w_{d_{N,1}}}$  and  $\tilde{\mathbf{f}} = \frac{\tilde{w}_{d_{q,p}}}{\tilde{w}_{d_{N,1}}}$  where  $q = 1, 2, \dots, N$  and  $p = 1, 2, \dots, \frac{n}{2^q}$  for every  $q$ , we can easily verify that  $\mathbf{f} = \tilde{\mathbf{f}}$ . Thus our effort to capture the intrinsic relation between the sample points of the actual curve and transformed curve is found to be obtained through the above said ratio of the vectors of wavelet detailed coefficients. Therefore we justified that the vector  $\mathbf{f} = \tilde{\mathbf{f}}$  can be called as TIFV of any space curve. The proposed TIFV of various curves are illustrated in next section. The algorithm for the computation of proposed TIFV is as follows:

**Step 1.** Get the equally spaced sample points  $(x_i, y_i, z_i)$  for  $i = 1, 2, \dots, n$  of the space curve.

**Step 2.** Collect the  $x$  components say  $(x_1, x_2, \dots, x_n)$ , the  $y$  components  $(y_1, y_2, \dots, y_n)$  and  $z$  components  $(z_1, z_2, \dots, z_n)$  as three vectors of  $n$  dimension

**Step 3.** Compute the first two principal components of the vectors given in step 2.

**Step 4.** Compute the componentwise wavelet transform of both the principal components given in step 3.

**Step 5.** Rearrange the pairs of wavelet coefficients of  $x$  and  $y$  in order.

**Step 6.** Calculate the ratio by dividing all the wavelet detailed coefficients by the last level wavelet detailed coefficient.

Step 7. Get the scaled, rotated and translated sample points of the given curve.

Step 8. Repeat the steps 2, 3, 4, 5 and 6.

The proposed TIFV of various curves are illustrated in next section.

#### 4. Illustrated examples

We present the computation of proposed TIFV of some of the sample curves in this section. For this purpose, we consider the sample points of actual curve and their transformations. The parametric curves  $x(t) = \cos(t)$ ,  $y(t) = \sin(t)$ ,  $z(t) = t$  and  $x(t) = t$ ,  $y(t) = t^2$ ,  $z(t) = t^3$  are considered for the study so that to justify the invariance property of the computed parameter for various types of curves. The actual and scaled, rotated and translated version of the curves considered above are depicted in Figure 1, Figure 2 respectively. We have used Haar wavelet and Daubechies wavelet of fourth order for the computation [2, 6]. We take 64 equally spaced sample points. We have implemented the computations using MATLAB R2013a. We have carried out all the six levels of wavelet transform for both the sets of points obtained by PCA. The required parameters of all the considered curves are obtained by using all the two wavelets. Despite these facts the wavelet detailed coefficients of the points obtained by dimension reduction of  $x(t) = \cos(t)$ ,  $y(t) = \sin(t)$ ,  $z(t) = t$  by Haar, and  $x(t) = t$ ,  $y(t) = t^2$ ,  $z(t) = t^3$  by Daubechies 4. only are presented in Table 1 and Table 2 respectively. Further, it is to be noted that the computational details of the last three levels only are given in the tables.

We briefly discuss the computation of proposed TIFV for  $x(t) = \cos(t)$ ,  $y(t) = \sin(t)$ ,  $z(t) = t$  by using Haar. We take 64 equally spaced sample

points of  $x(t) = \cos(t)$ ,  $y(t) = \sin(t)$ ,  $z(t) = t$ ,  $0 \leq t \leq 63$ . We also obtained the scaled, rotated and translated points of the parametric curve using  $s = 2$ ,  $\alpha = \beta = \gamma = 30^\circ$ ,  $t_x = 2$ ,  $t_y = 3$  and  $t_z = 4$ . We obtain the atypical wavelet detailed coefficients of the principal components of the sample points. On our effort to identify the relationship between both the sets of sample points, nothing is found to be extracted evidently from either the sample points or from their wavelet coefficients. This observation is not as devastating to our plans as it appears because it turns out that the proposed TIFV leads to the desired results. This TIFV is obtained by dividing all the wavelet detailed coefficients by last level wavelet detailed coefficient [9] (-45.2564, 0.20782) and (-90.5085, 0.41529) of both the sets of actual and transformed principal components. It is observed that the vectors  $\mathbf{f}$  and  $\tilde{\mathbf{f}}$  are the same. Thus these vectors capture the intrinsic relationship between both the sets of actual and transformed sample points and hence the resulting vector  $\mathbf{f} = \tilde{\mathbf{f}}$  can be defined as TIFV of a space curve.

#### 1. Conclusion

The relationship between the sample points of a space curve and scaled, rotated and translated sample points are studied in our work. However plethora of attempts has been made on planar curves using Fourier and wavelet transforms. It is observed that the strategy adapted for the planar curve is not suitable for the curves in space.

**Table1.**  $x(t) = \cos(t), y(t) = \sin(t), z(t) = t$

No	$\mathbf{W}_{d(q,p)}$	$\tilde{\mathbf{W}}_{d(q,p)}$	$\mathbf{f}/\tilde{\mathbf{f}}$
q=6,p=1	(-45.2564, 0.20782)	(-90.5085, 0.41529)	(1.00000, 1.00000)
q=5,p=1	(-45.2564, -0.20782)	(-90.5085, -0.41596)	(0.99996, 0.009184)
q=5,p=2	(-15.9993, 0.54093)	(-31.9971, 1.08198)	(0.35357, -0.01033)
q=4,p=1	(-16.0002, -0.59097)	(-31.9988, -1.18193)	(0.35348, 0.01468)
q=4,p=2	(-16.0002, 0.59097)	(-31.9988, 1.18187)	(0.35359, -0.01143)
q=4,p=3	(-15.9993, -0.54093)	(-31.9971, -1.08165)	(0.35346, 0.01358)
q=4,p=4	(-5.65978, -0.33037)	(-11.3190, -0.66136)	(0.12502, 0.00787)

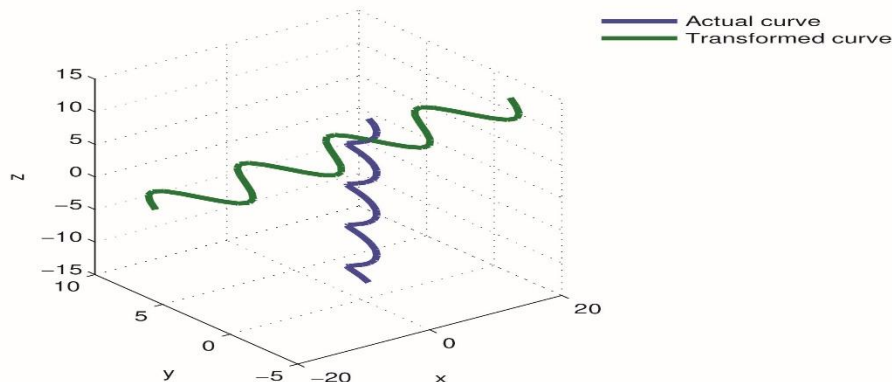


Fig. 1:  $x(t) = \cos(t), y(t) = \sin(t), z(t) = t$

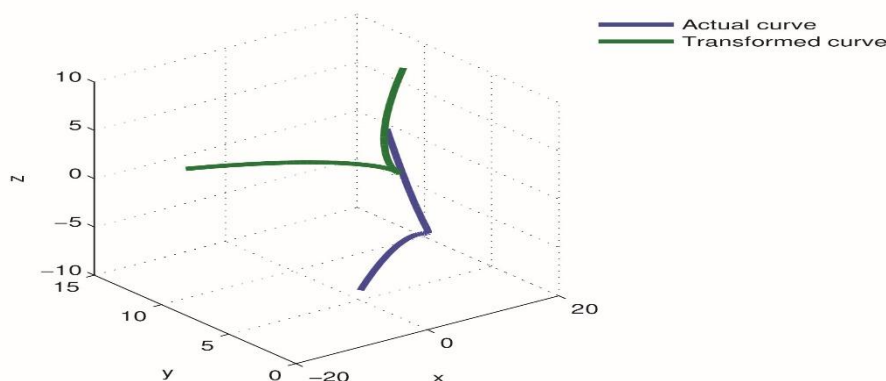


Fig. 2:  $x(t) = t, y(t) = t^2, z(t) = t^3$

Table 2.  $x(t) = t, y(t) = t^2, z(t) = t^3$ .

No	$W_{d(q,p)}$	$\tilde{W}_{d(q,p)}$	$f/\tilde{f}$
q=6,p=1	(225558, 1416.94)	(451107, 2833.82)	(1.00000, 1.00000)
q=5,p=1	(-145768, 493.263)	(-291530, 986.504)	(-0.64622, 0.00625)
q=5,p=2	(421936, -352.222)	(843855, -704.429)	(1.87055, -0.0133)
q=4,p=1	(-13491.1, 255.669)	(-26980.6, 511.327)	(-0.05980, 0.00151)
q=4,p=2	(22834.7, -15.6322)	(45668.4, -31.2638)	(0.10123, -0.00071)
q=4,p=3	(-3114.37, -15.2144)	(-6228.59, -30.4281)	(-0.01381, -0.00002)
q=4,p=4	(214463, -350.081)	(428917, -700.147)	(0.95076, -0.00752)

Therefore we made our effort to reduce the dimension of the space curve using PCA. The required relationship is not evident even with the wavelet coefficients of the principal components. However, we could extract these intrinsic relationships by a specific ratio of the wavelet detailed coefficients of principal components. This study is accomplished by using atypical orthogonal wavelet coefficients for both the set of principal

components of the sample points. In fact, we have established these relationships by mathematical analysis. Our results are illustrated with few continuous space curves. It is interesting to state that the proposed TIFV is can be useful as a feature for the study related to image classification. We have used various orthogonal wavelets to perform atypical wavelet transform.

The results are found to be independent of the wavelets used.

#### References

- [1] S. Anusha, A. Sriram, and T. Palanisamy. A comparative study on decomposition of test signals using variational mode decomposition and wavelets. *International Journal on Electrical Engineering and Informatics*, 8(4):886, (2016). doi:/10.15676/ijeei.2016.8.4.13.
- [2] C. Heil. Ten lectures on wavelets (ingrid daubechies). *SIAM Review*, 35(4):666–669, 1993.
- [3] M. W. Frazier. *An introduction to wavelets through linear algebra*. Springer Science & Business Media, 2006.
- [4] F. Freudenstein. Harmonic analysis of crank-and-rocker mechanisms with application. *Journal of Applied Mechanics*, 26(4):673–675, (1959).
- [5] S. Ganga, M. K. Panthangi, and T. Palanisamy. Numerical solution of blasius viscous flow problem using wavelet galerkin method. *International Journal for Computational Methods in Engineering Science and Mechanics*, pages 1–7, (2020). doi:/10.1080/15502287.2020.1772903
- [6] R. Gokul, A. Nirmal, G. Dinesh Kumar, S. Karthic, and T. Palanisamy. A combined wavelet and variational mode decomposition approach for denoising texture images. In *International Conference on Computer Vision and Image Processing*, pages 50–62. Springer, (2020). doi:/10.1007/978-981-16-1092-9-5
- [7] K.-C. Hung, T.-K. Truong, J.-H. Jeng, and J.-T. Yao. Uniqueness wavelet descriptor for plane closed curves. In *1997 IEEE Pacific Rim Conference on Communications, Computers and Signal Processing, PACRIM. 10 Years Networking the Pacific Rim, 1987-1997*, volume 1, pages 294–297. IEEE, (1997).doi:/10.1109/PACRIM.1997.619 958.
- [8] I. T. Jolliffe and J. Cadima. Principal component analysis: a review and recent developments. *Philosophical Transactions of the Royal Society A: Mathematical, Physical and Engineering Sciences*, 374(2065):20150202, (2016). doi:/10.1098/rsta.2015.0202.
- [9] W. Liu, J. Sun, B. Zhang, and J. Chu. Wavelet feature parameters representations of open planar curves. *Applied Mathematical Modelling*, 57:614–624, (2018). doi:10.1016/j.apm.2017.05.035.
- [10] J. Ma and Y. Yuan. Dimension reduction of image deep feature using pca. *Journal of Visual Communication and Image Representation*, 63:102578, (2019). doi:/10.1016/j.jvcir.2019.102578.
- [11] J. McGarva and G. Mullineux. A new methodology for rapid synthesis of function generators. *Proceedings of the Institution of Mechanical Engineers, Part C: Journal of Mechanical Engineering Science*, 206(6):391–398, (1992). doi:/10.1243/pimeproc19922061460
- [12] J. McGarva and G. Mullineux. Harmonic representation of closed curves. *Applied Mathematical Modelling*, 17(4):213–218, (1993). doi:/10.1016/0307-904x(93)90109-t.
- [13] J. R. McGarva. Rapid search and selection of path generating mechanisms from a library. *Mechanism and machine theory*, 29(2):223–235, (1994). doi:/10.1016/0094-114x(94)90032-9.
- [14] G. Mullineux. Atlas of spherical four-bar mechanisms. *Mechanism and machine theory*, 46(11):1811–1823, (2011). doi:/10.1016/j.mechmachtheory.2011.06.0 01.
- [15] T. Palanisamy and J. Ravichandran. A wavelet-based hybrid approach to estimate variance function in heteroscedastic regression models. *Statistical Papers*, 56(3):911–932, (2015). doi:/10.1007/s00362-014-0614-6.
- [16] A. Sridharan, R. A. AS, and S. Gopalan. A novel methodology for the

- classification of debris scars using discrete wavelet transform and support vector machine. *Procedia Computer Science*, 171:609–616, (2020).doi:/10.1016/j.procs.2020.04.066.
- [17] J. Sun and J. Chu. Fourier series representation of the coupler curves of spatial linkages. *Applied Mathematical Modelling*, 34(5):1396–1403, (2010). doi:/10.1016/j.apm.2009.08.030
- [18] J. Sun, W. Liu, and J. Chu. Synthesis of spherical four-bar linkage for open path generation using wavelet feature parameters. *Mechanism and Machine Theory*, 128:33–46, (2018). doi:/10.1016/j.mechmachtheory.2018.05.008Get.
- [19] Q. M. Tieng, W. W. Boles, and M. Deriche. Space curve recognition based on the wavelet transform and string-matching techniques. In *Proceedings, International Conference on Image Processing*, volume 2, pages 643–646. IEEE, (1995).
- [20] Y. Uesaka. A new fourier descriptor applicable to open curves. *Electronics and Communications in Japan (Part I: Communications)*, 67(8):1–10, (1984). doi:/10.1002/ecja.4400670802
- [21] D. Vignesh, T. Palanisamy, et al. Invariance of geometry of planar curves using atypical wavelet coefficients. *Journal of Applied Science and Engineering*, 26(5):731–737, (2022). doi.org/10.6180/jase.20230526(5).0014.
- [22] J. Wu, Q. Ge, and F. Gao. An efficient method for synthesizing crank-rocker mechanisms for generating low harmonic curves. In *ASME 2009 International Design Engineering Technical Conferences and Computers and Information in Engineering Conference*, pages 531–538. American Society of Mechanical Engineers Digital Collection, (2009). doi:/10.1115/detc2009-87140.
- [23] C. Yue, H.-J. Su, and Q. J. Ge. A hybrid computer-aided linkage design system for tracing open and closed planar curves. *Computer-Aided Design*, 44(11):1141–1150, (2012). doi:/10.1016/j.cad.2012.06.004